Article

Osmotic heat engine using thermally responsive ionic liquids

Yujiang Zhong, Xinbo Wang, Xiaoshuang Feng, Selvedin Telalovic, Yves Gnanou, Kuo-Wei Huang, Xiao Matthew Hu, and Zhiping Lai

Environ. Sci. Technol., **Just Accepted Manuscript** • DOI: 10.1021/acs.est.7b02558 • Publication Date (Web): 11 Jul 2017

Osmotic heat engine using thermally responsive ionic liquids

Yujiang Zhong[a†], *Xinbo Wang*[a†], *Xiaoshuang Feng*[a], *Selvedin Telalovic*[a], *Yves Gnanou*[a], *Kuo-Wei Huang*[a], *Xiao Hu*[bc*], *Zhiping Lai*[a*]

[a]Division of Physical Science and Engineering, King Abdullah University of Science and Technology, Thuwal, 23955-6900, Saudi Arabia.

[b]School of Material Science and Engineering, Nanyang Technological University, Singapore.

[c]Environmental Chemistry and Materials Centre, Nanyang Environment and Water Research Institute.

[†]These authors contribute equally.

ABSTRACT: The osmotic heat engine (OHE) is a promising technology for converting low grade heat to electricity. Most of the existing studies have focused on thermolytic salt systems. Herein, for the first time, we proposed to use thermally responsive ionic liquids (TRIL) that have either an upper critical solution temperature (UCST) or lower critical solution temperature (LCST) type of phase behavior as novel thermolytic osmotic agents. Closed-loop TRIL-OHEs were designed based on these unique phase behaviors to convert low grade heat to work or electricity. Experimental studies using two UCST-type TRILs, protonated betaine bis(trifluoromethyl sulfonyl)imide ([Hbet][Tf_2N]) and choline bis(trifluoromethylsulfonyl)imide ([Choline][Tf_2N]) showed that (1) the specific energy of the TRIL-OHE system could reach as

high as 4.0 times that of the seawater and river water system, (2) the power density measured from a commercial FO membrane reached up to 2.3 W/m^2, and (3) the overall energy efficiency reached up to 2.6% or 18% of the Carnot efficiency at no heat recovery and up to 10.5% or 71% of the Carnet efficiency at 70% heat recovery. All of these results clearly demonstrated the great potential of using TRILs as novel osmotic agents to design high efficient OHEs for recovery of low grade thermal energy to work or electricity.

TOC ART

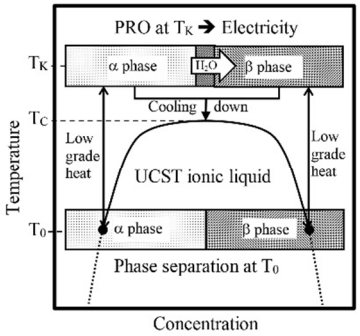

KEYWORDS: Osmotic heat engine, thermally responsive ionic liquid, low grade heat, pressure-retarded osmosis, osmotic pressure

INTRODUCTION

Low grade heat with a temperature below 120 °C is available in abundance not only from various industrial processes but also from solar heating, geothermal energy, nuclear power and so on. It is estimated that more than 50% of the energy in industry eventually ends up as low grade heat due to process inefficiency.[1, 2] The concept of using OHE to recover low grade heat was first proposed by Loeb in 1975 based on a pressure-retarded osmosis (PRO) process that uses a semipermeable membrane to harvest the salinity gradient energy (SGE) and then uses low grade heat to regenerate the salinity gradient.[3] Compared with other technologies that are currently under development such as the Rankine cycle, Sterling engines and solid-state devices based on

the Seebeck effect, and so on, OHE is easy scalability, requires no addition of chemicals, and produces zero discharge.[1, 4]

The osmotic agent is the working medium of OHE. The first proposed osmotic agent is simply a sodium chloride solution. Due to a small change in the boiling point of NaCl solution with concentration, this approach is limited by its low efficiency.[5] Hence, most OHE studies have focused on thermolytic salt systems for which solubility changes dramatically with temperature.[6] The most famous example is probably the NH_3-CO_2 system developed by Elimelech et al. By using a conventional steam stripping system to regenerate the solution, the overall efficiency was improved to around 1%.[7] A broader range of OHE devices include also electrochemical concentration cells and capacitive mixing or mixing entropy batteries.[8-16] Ammonia has a low molecular weight, which on the one hand offers the advantage of high solubility and therefore a high power density, whereas on the other hand it causes a high membrane cross-over rate which reduces the efficiency. Furthermore, its toxicity and unpleasant odor make it difficult to handle. Hence, developing a good osmotic agent is still a large challenge in OHE development.

Herein, we propose a novel idea of using thermally responsive ionic liquids (TRILs) as the osmotic agent. Ionic liquids (ILs) are electrolytes with a melting point typically lower than room temperature.[17] They are often considered as green solvents and have found broad applications in catalysis, separation, food and pharmaceutical processes, and so on.[17, 18] Thermally responsive ionic liquids have phase diagrams with either an upper critical solution temperature (UCST) or a lower critical solution temperature (LCST). In our previous reports we demonstrated that both UCST- and LCST-types of ILs can be used as novel draw solutions in the forward osmosis processes for water desalination.[19, 20] As an osmotic agent, ILs have a number of advantages. ILs are electrolytes that can dissociate into ions and generate higher osmotic pressure. ILs are

typically large molecules, which minimize the crossover issue. ILs are liquids. The phase separation is much faster than other thermally responsive agents such as polymers, and it will not cause membrane fouling or flow blocking.[21] ILs have high boiling points and low vapor pressures, reducing the potential material loss during heating/cooling cycles. Hence, TRILs are expected to be a very promising type of osmotic agent. The disadvantages of ILs are high cost, high viscosity, and low diffusion coefficient that may leads to large concentration polarization.

The specific energy (SE) and power density (PD) are two figure-of-merit parameters for an OHE. The specific energy is determined by the Gibbs energy of mixing, which is determined by the maximum osmotic pressure difference. Power density is a property primarily related to membrane performance, but it is also related to the maximum osmotic pressure difference because from process design studies it was found that the maximum power density occurs typically at the condition when the retarded pressure is equal to half of the maximum osmotic pressure difference.[22] Hence, the maximum osmotic pressure difference is a critical value. Herein, we use two UCST-type ILs, protonated betaine bis(trifluoromethylsulfonyl)imide ([Hbet][Tf_2N]) and choline bis(trifluoromethylsulfonyl)imide ([Choline][Tf_2N]), to illustrate the OHE concept and to demonstrate the potential performance from osmotic pressure measurements.

MATERIALS AND METHODS

Materials. [Hbet][Tf_2N] (> 99%) and [Choline][Tf_2N] (> 99%) were purchased from Shanghai Chengjie Chemical Co., Ltd. Sodium chloride (>99.5%) was purchased from Sigma-Aldrich. All chemicals were used as received without further purification. Water purified by a Milli-Q (Milli Pore) system was used as fresh water in all experiments.

Measurements. The primary method to measure the concentration of IL and NaCl solutions is through conductivity (Thermo Scientific™ Orion™ 5 STAR and Orion™ 013005MD Conductivity Cell). The solution needs to be diluted to low down the concentration to the linear response region. For mixtures containing both IL and NaCl, the conductivity measurement gives the total ionic concentration. In this case the concentration of NaCl is determined through measurement of chloride by an Aquakem 250 photometric analyzer (Thermo Scientific). The concentration of IL was also verified by two methods: (1) UV-vis spectra (Cary 5000) if it is UV sensitive, and (2) for the β phase (IL-rich phase), the water content was measured by a standard Karl Fischer Titrator (Mettler Toledo, C30X). The heat capacity of IL solution was detected by a differential scanning calorimetry (Mettler Toledo DSC 1). The heat of mixing was measured by a C80 calorimeter (Setaram). The solution density was determined from weight and volume measurements. The osmotic pressure was measured by a custom-designed forward osmosis setup as shown in Fig. 1. The setup contains two glass chambers, one filled with IL solution and the other with NaCl solution. A polyamide reverse osmosis membrane (Toray, UTC-73AC), which has a good salt rejection rate, was placed in the middle of the two chambers. The whole setup was maintained at the working temperature T_K by immersion in a water bath. An equivalent NaCl solution having the same osmotic pressure as the IL solution was found by adjusting the concentration of the NaCl solution until water transport through the membrane in both ways was observed. The concentrations of NaCl and IL in both solutions were measured after the experiment to ensure that the leakage rate across the membrane was negligible.

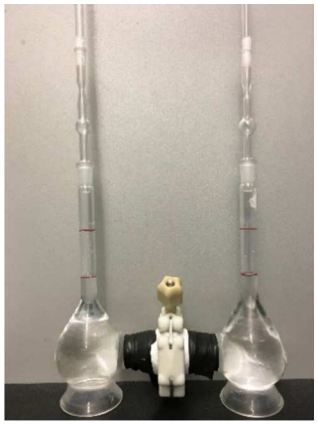

Figure 1. A custom-designed apparatus for osmotic pressure measurement.

RESULTS AND DISCUSSION

Fig. 2a shows the phase diagrams of the two ILs. Both phase diagrams exhibit a critical temperature T_c, above which the IL is completely miscible with water but under which the mixture separates spontaneously into a water-rich phase (denoted as α phase) and an ionic liquid–rich phase (denoted as β phase).

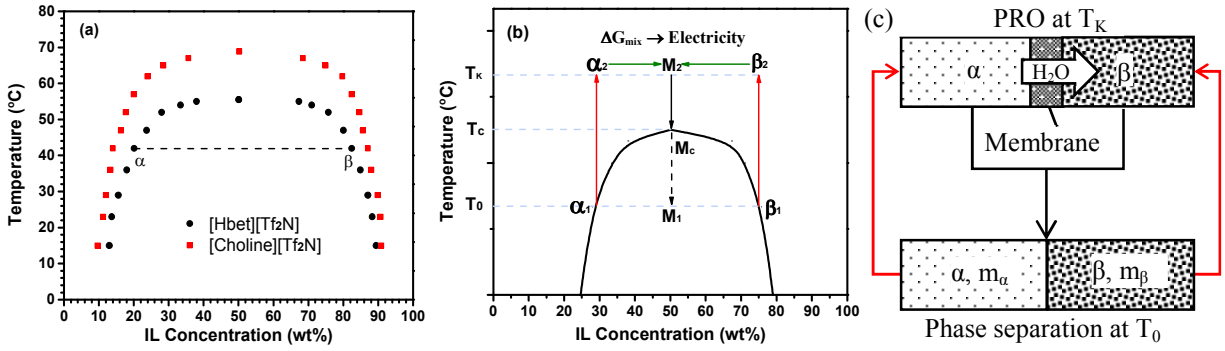

Figure 2. (a) Phase diagrams of [Hbet][Tf_2N] and [Choline][Tf_2N] aqueous solutions; (b) Illustration of an TRIL-OHE loop on the phase diagram; (c) illustration of an TRIL-OHE by a PRO process.

Based on the UCST phase behavior, a novel closed-loop TRIL-OHE was designed as illustrated in Fig. 2b and Fig. 2c. The most studied pressure-retarded osmosis (PRO) process was used to

demonstrate the energy conversion process in Fig. 2c, but other commonly studied processes such as reverse electro dialysis (RED) and capacitance mixing (CM) can also be used. All of these processes have 100% ideal efficiency if conducted reversibly[4, 11, 23]. The TRIL-OHE loop includes three stages. The first stage starts from a temperature T_0 (for example, room temperature 23°C) which should be lower than the critical temperature T_c. The equilibrium pair of α and β solutions obtained at T_0 are heated separately to a working temperature T_K that should be above the critical temperature and then placed in the two sides of a semipermeable membrane which allows the transport of water only. The second stage is the PRO process that is conducted reversibly at T_K by applying a pressure equal to the osmotic pressure difference of the two solutions to the β phase. Water is drawn from the α phase to the β phase by osmotic pressure which increases the volume of the β phase and in turn generates either mechanical work or electricity. Because T_K is above the critical temperature, a single phase will eventually form after mixing. The mixture is then cooled in the third stage to the initial temperature T_0, regenerating the original two phases. Table 1 lists all the operation parameters of the TRIL-OHE loop assuming to generate 1000 kg mixture after the PRO process.

Table 1. Operation conditions of the TRIL-OHE loop for the two IL systems

IL	Tc (°C)	Wc (wt%)	μ (Pa·s)	T_0 (°C)	Wα (wt%)	$W_β$ (wt%)	$m_α$ (kg)	$m_β$ (kg)	T_K (°C)
[Hbet][Tf_2N]	55.6	50.1	0.030	23.0	13.7	88.3	512.06	487.94	60.0
[Choline][Tf_2N]	68.9	50.2	0.024	23.0	11.2	90.7	509.43	490.57	74.0

T_C, critical temperature; W_C, critical concentration; μ, viscosity measured at T_K; T_0, initial temperature; $W_α$, concentration of α phase at T_0; $W_β$, concentration of β phase at T_0; $m_α$, amount of α phase; $m_β$, amount of β phase; T_K, working temperature.

The maximum energy that can be extracted out of SGE is the Gibbs mixing energy, which in principle can be calculated from thermodynamic models.[24-26] Most of these models, however,

contain empirical parameters which are not available due to the limit of experimental data. Hence, herein the Gibbs mixing energy was obtained through experimental measurement of the osmotic pressure based on the following equation:

$$\Delta G_{mix} = -\int_0^V \Delta\pi dV \quad (1)$$

where $\Delta\pi$ is the osmotic pressure difference between the α and β phases, and V is the total amount of water drawn from the α to β phase during the PRO process. Unfortunately, the osmotic pressure of TRILs cannot be measured by commercial osmometers because they typically utilize colligative properties such as the decrease in melting point. Therefore, a custom-designed forward osmosis (FO) setup was built as shown in Fig. 1.

The mechanism of measurement was to use the sodium chloride solution as a reference to find the equivalent osmotic pressure of the ionic liquid solution by observing the transport of water in a trial-and-error fashion. If the osmotic pressures of the two solutions are equal, then no water should pass through the membrane. Otherwise water will be extracted from the solution with a lower osmotic pressure to the solution with the higher one. During the experiment, one container was filled with sodium chloride solution with a known concentration while the other was filled with an ionic liquid solution with a known concentration. The whole setup was immerged into a circulation bath to maintain the temperature at the working temperature T_K, which was selected as approximately 5 °C above the critical temperature in this study. The osmotic pressures of the NaCl solution at different salt concentrations are available from a reference[27] and shown in Fig. 3a.

Table 2 shows an example of how the equivalent osmotic pressure of a 1.14 M (40 wt%) [Hbet][Tf_2N] solution was determined at T_K = 60 °C. A 1.035 M NaCl solution was first tested.

After 22 hours, it was found that 0.792 g of water was extracted from the ionic liquid to the NaCl solution, indicating that the equivalent osmotic pressure of the ionic liquid solution should be lower. Hence, the concentration of the NaCl solution was lowered to 1.0 M, then to 0.937 M, and finally to 0.92 M. The amount of water extracted from the ionic liquid to NaCl became increasingly lower until a reverse transport of water was observed at the last measurement. The average value of the last two measurements was used as the final result. The error of measurement of this approach is estimated to be less than 1%. Table 2 also showed the total conductivity (κ) of the solutions before and after each trial, and the conductivity in parenthesis showed the contribution from the minor component, i.e. NaCl in IL solution or IL in NaCl solution. As the data shown, the changes in total conductivities before and after each trial matched very well with the direction of water transport, verifying the accuracy of our measurements. For example, when water was extracted from IL solution to NaCl solution, the conductivity of IL solution increased while that of NaCl solution decreased, or vice versa. The minor component is due to leakage during experiment. Their conductivities were less than 0.5% of the total conductivity, indicating that the leakage rate was very small. Based on the FO measurements, the equivalent osmotic pressure of the two ILs at different IL concentrations are shown in Fig. 3b.

Table 2. Osmotic pressure detection for a 1.14 M (40 wt%) [Hbet][Tf2N] water solution at 60 °C

Trial	IL Conc. (M)	NaCl Conc. (M)	Time (h)	Water Pass (h)	Water Flux (LMH)	IL side (dilute 5 times)			NaCl side (dilute100 times)		
						κ_before (ms/cm)	κ_after (ms/cm)		κ_before (μs/cm)	κ_after (μs/cm)	
1	1.14	1.035	22	0.792	0.068	19.57	20.27	(0.047)	1322	1307	(1.10)
2	1.14	1.000	22	0.509	0.044	20.27	20.94	(0.046)	1196	1182	(1.19)
3	1.14	0.937	21	0.057	0.006	20.03	20.12	(0.043)	1013	1005	(1.14)
4	1.14	0.920	20	-0.055	-0.006	20.06	19.98	(0.042)	965	974	(1.15)

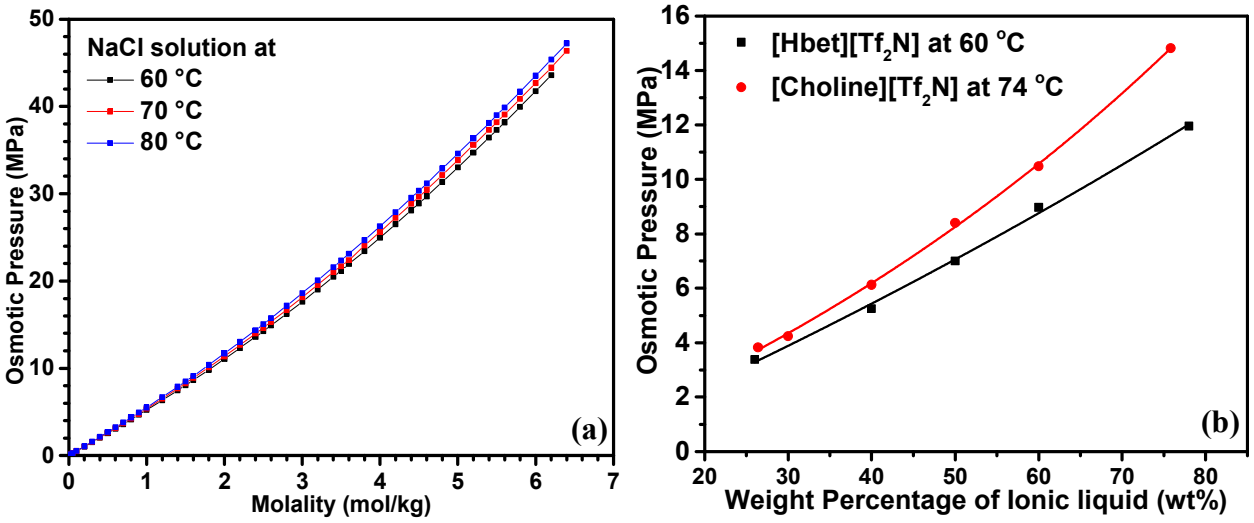

Figure 3. (a) Osmotic pressure of NaCl aqueous solution at different molality and temperature. Data obtained from a reference;[27] (b) osmotic pressures of the two IL solutions at different weight percentage measured at T_K.

The Gibbs mixing energy can then be calculated as follows. Assuming *f(x)* is the function of the equivalent osmotic pressure at weight percentage *x*, which can be data fitted from Fig. 3b, and V is the amount of water extracted from the α phase to the β phase, then the osmotic pressure difference of the two phases Δπ can be calculated from the following equation:

$$\Delta\pi = f\left(\frac{m_\beta W_\beta}{m_\beta + \rho V}\right) - f\left(\frac{m_\alpha W_\alpha}{m_\alpha - \rho V}\right) \quad (2)$$

where m_α, W_α, m_β, and W_β are the amount and the weight percentage of the α and β phases, respectively, and ρ is the density of pure water. The total amount of ionic liquid $m_\alpha+m_\beta$ was fixed at 1000 kg. The concentrations of the α and β phases were determined by the initial temperature T_0. It was further assumed that after mixing the mixture had the same concentration as the critical concentration. Then m_α and m_β in Equation (2) can be calculated accordingly. Fig. 4a shows the relationship of Δπ vs. V of the two ionic liquid systems when the initial temperature was fixed at room temperature (23 °C). The areas under the curves are the maximum

Gibbs mixing energy per 1000 kg of the total mixed ionic liquid solutions, or the specific energy, SE, of the system. Fig. 4b shows the specific energies at different initial temperatures. Obviously, the lower the initial temperature, the higher is the concentration difference between the α and β phases and thus the higher the specific energy. At 23 °C, the specific energy was approximately 2500 kJ/t for [Hbet][Tf_2N] and 3700 kJ/t for [Choline][Tf_2N]. It is worthy to note that the specific energy between regular seawater and river water was approximately 912 kJ/t.[28] Thus, the specific energy of the two ionic liquids are approximately 1.74 and 3.06 times higher. The specific energy can be further optimized in terms of the mass ratio of two phases. Fig. 4c shows the specific energy at different $m_\beta/(m_\alpha+m_\beta)$. The optimal ratio was found to be 1.157 for [Hbet][Tf_2N] and 1.075 for [Choline][Tf_2N]. Interestingly, these ratios were exactly the same values after mixing when the concentration of the mixture was equal to the critical concentration.

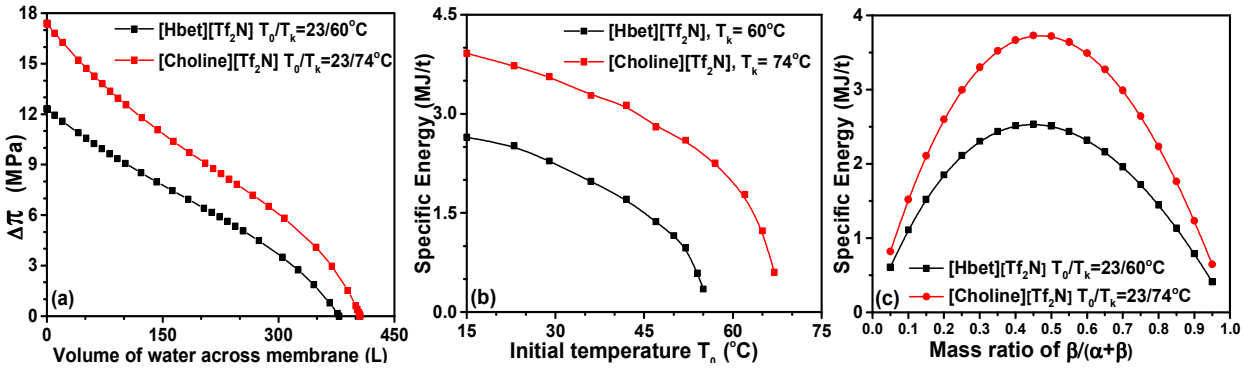

Figure 4. (a) Osmotic pressure difference at different amounts of water drawn across the membrane from the α to β phase at the working temperature T_K, (b) specific energy at different initial temperature T_0, and (c) the specific energy at different $m_\beta/(m_\alpha+m_\beta)$ ratios from the room temperature α/β pair.

Power density (PD) is a measure of the energy generated per unit time and unit membrane area. It is an important performance index of the PRO process. The gross power density can be calculated as the product of water flux J_w and the hydraulic pressure difference ΔP.

$$PD = J_w \Delta P \quad (3)$$

In the ideal case,

$$PD = A(\Delta\pi - \Delta P)\Delta P \quad (4)$$

It reaches the maximum when $\Delta P = \pi_{max}/2$[22] and thus,

$$\mathrm{PD}_{max} = \frac{1}{4} A \Delta\pi_{max}^2 \quad (5)$$

The maximum osmotic pressure difference $\Delta\pi_{max}$ in Equation (5) can be read directly from Fig. 4a, but the water permeability coefficient, A, is a membrane property. From the osmotic pressure measurements, it was found that the commercial HTI© membrane, which is made from cellulose acetate and often used for FO or PRO processes, was not stable in the ionic liquid. Hence, during the osmotic pressure measurement a commercial polyamide membrane (Toray, UTC-73AC) that is typically used for reverse osmosis was used as the semipermeable membrane. The membrane was found to be very stable even after hundreds of hours of testing. It has a good salt rejection rate, which is beneficial for our fundamental studies to obtain the maximum Gibbs mixing energy. However, the disadvantage of this membrane is its low water flux which will lead to low power density. Another commercial FO membrane HTI OsMem™ TFC-ES Membrane was found stable and gave relatively higher water flux. The measured water flux between the α and β phases were 1.71 LMH for [Hbet][Tf_2N] at 60 °C and 1.95 LMH for [Choline][Tf_2N] at 74 °C. Using the ideal equation (4) the A values were calculated to be 0.014 LMH/bar for [Hbet][Tf_2N] and 0.011 LMH/bar for [Choline][Tf_2N]. Correspondingly, the maximum power density calculated from Equation (5) gives 1.5 W/m^2 for [Hbet][Tf_2N] and 2.3 W/m^2 for

235 [Choline][Tf_2N]. These values are comparable to many reports for the seawater-river water
236 system.[29, 30] It should be noted that the A values were estimated without considering
237 concentration polarization, which is a well-known issue in FO and PRO processes that leads to
238 reduced driving force across the membrane.[31] Hence, the intrinsic A values without centration
239 polarization should be larger and the corresponding power density should be higher.[32] Recently,
240 a number of high-flux polyamide type of thin film composite (TFC) membranes have been
241 successfully developed for the PRO process with A value reached up to 1 LMH/bar.[33] Hence,
242 there should be a big room for further improvement of the power density for the TRIL-OHE
243 system in order to meet the economic requirements.[34]

244 The temperature vs. entropy of the TRIL-OHE cycle is shown in Fig. 5. In the first stage, the
245 system requires $Q_\alpha + Q_\beta$ amount of heat to increase the temperature from T_0 to T_K. The entropy
246 of the system will increase with temperature roughly by amount of $\left(C_P^\alpha + C_P^\beta\right) \ln \frac{T_K}{T_0}$. In the
247 second stage, the PRO process operates isothermally, thus temperature will keep constant, but
248 since it is a spontaneous mixing process, so entropy will increase by amount of ΔS_{mix}. The
249 system in this stage may adsorb or release heat depending on the heat of mixing ΔH_{mix}. In the
250 third step, the mixture is cooled down from T_K to T_0, and the system recovers back to the original
251 state. The heat released from the third stage, Q_m, should be able to be recovered by a heat
252 exchanger coupling with the first stage.

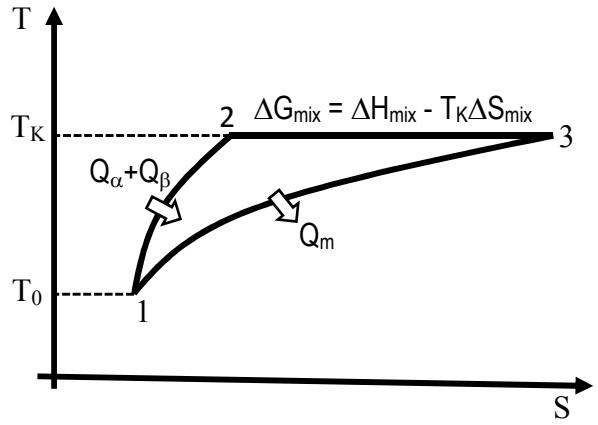

Figure 5. Temperature-Entropy diagram of a TRIL-OHE cycle

Based on the above T-S diagram, the energy balance of each step and the overall energy efficiency can be calculated as below. The heat required for stage one is calculated by,

$$Q_\alpha + Q_\beta = m_\alpha \int_{T_0}^{T_K} C_p^\alpha dT + m_\beta \int_{T_0}^{T_K} C_p^\beta dT \quad (6)$$

and the heat released in stage three is calculated by,

$$Q_m = (m_\alpha + m_\beta) \int_{T_0}^{T_K} C_p^m dT \quad (7)$$

where C_p^α, C_p^β and C_p^m are the heat capacities of the α phase, β phase and mixture, respectively, and their values at different temperatures are shown in Fig. 6a and 6b. It is noted that the mixture will undergo phase separation during cooling. Hence, C_p^m is the overall value of the two phases. The energies involved in each step of the TRIL-OHE loop are listed in Table 3.

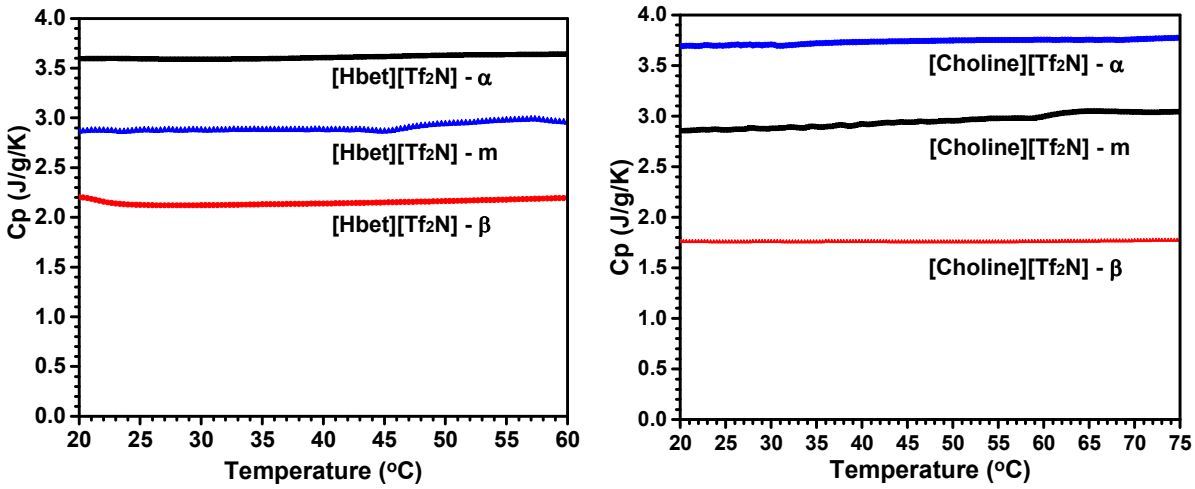

265

266 **Figure 6.** (a) Heat capacity of [Hbet][Tf2N] in the process temperature range, (b) Heat capacity

267 of [Choline][Tf2N] in the process temperature range.

268 **Table 3.** Energy at each step of the TRIL-OHE loop. All calculations are based on 1000 kg of

269 mixture and the operation conditions listed in Table 1.

IL	ΔGmix (kJ)	ΔHmix (kJ)	Qα+Qβ (kJ)	Qm (kJ)
[Hbet][Tf2N]	-2.52×10^{3}	44	1.072×10^{5}	1.075×10^{5}
[Choline][Tf2N]	-3.73×10^{3}	-190	1.412×10^{5}	1.507×10^{5}

270

271 It is interesting to find $(m_\alpha + m_\beta)C_P^m \approx m_\alpha C_P^\alpha + m_\beta C_P^\beta$, and $Q_m \approx Q_\alpha + Q_\beta$. It implies that

272 the heat released from the third stage can be largely recovered through a heat exchanger coupling

273 with the first stage. Assuming the recovery rate is η, then the overall energy efficiency is,

274 $$E = -\Delta G_{mix}/(Q_\alpha + Q_\beta - \eta Q_2 + \Delta H_{mix}) \quad (8)$$

275 Carnot efficiency is calculated by,

276 $$E_C = (T_K - T_0)/T_K \quad (9)$$

277 The Carnot efficiency for [Hbet][Tf2N] system is around 11.1% and for [Choline][Tf2N] system

278 around 14.7%. Fig. 7 shows the energy efficiency at different heat recovery rate. If assuming the

279 average temperature difference of the heat exchanger is about 10°C, it is estimated that about

70% heat of the [Hbet][Tf_2N] system and about 80% heat of the [Choline][Tf_2N] system can be recovered. As can be seen in Fig. 7, without heat recovery the energy efficiency is about 2.4% for [Hbet][Tf_2N] system and about 2.6% for [Choline][Tf_2N] system, or 21% and 18% of their Carnot efficiency, respectively. While at 70% heat recovery, the efficiencies can reach as high as 7.9% and 10.5%, or 71% and 71% of the Carnot efficiency for the two IL systems, respectively.

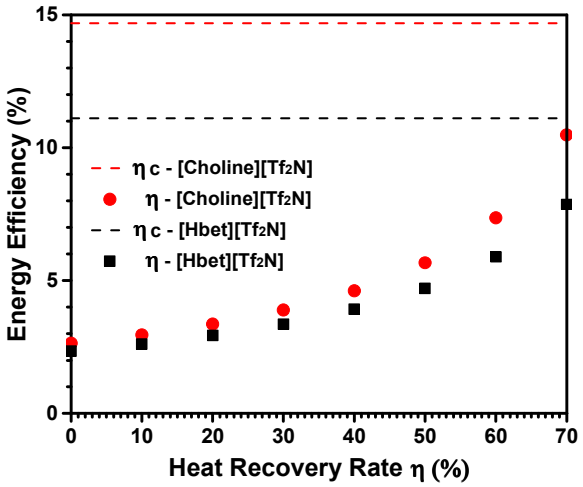

Figure 7. The energy efficiency at different heat recovery rate.

Based on the unique phase diagrams of two UCST type of ionic liquids, [Hbet][Tf_2N] and [Choline][Tf_2N], a novel closed-loop TRIL-OHE was designed to convert low grade thermal energy to electricity. The osmotic pressures of the two ionic liquids were measured using a custom-designed FO setup using NaCl solution as a reference. From the osmotic pressure data, the specific energy and the power density, two performance metric parameters of OHE, were estimated. The specific energy increases when the initial temperature decreases. When the initial temperature is set at room temperature (23 °C), the specific energy of the [Hbet][Tf_2N] system was around 2500 kJ/t and that of the [Choline][Tf_2N] system around 3700 kJ/t, which are 2.7 and 4.0 times the seawater and river water system, respectively. The maximum power density measured from a commercial FO membrane is about 1.5 W/m^2 for the [Hbet][Tf_2N] system and

2.3 W/m^2 for the [Choline][Tf_2N] system. The power density is obtained from a relatively low permeable membrane. There should be still a big room to improve the power density if highly permeable membranes are used. During the experiment, it was found that the cellulose acetate type of membranes were not stable in ionic liquid solutions, but this was not an issue for polyamide type of membranes. The temperature-entropy diagram of the TRIL-OHE loop was analyzed. A notable advantage of the TRIL-OHE was revealed from the energy balance, that is, the heat released from the cooling stage can be largely recovered. A rigorous energy balance showed without heat recovery the energy efficiency was about 2.4% or 21% of the Carnot efficiency for the [Hbet][Tf_2N] system, and about 2.6% or 18% of the Carnot efficiency for the [Choline][Tf_2N] system, while at 70% heat recovery, the energy efficiency increased to 7.9% or 71% of the Carnot efficiency and 10.5% or 71% of the Carnot efficiency for the two ionic liquid systems, respectively. All of these results clearly demonstrated the superior performance of the TRIL-OHE system. Therefore, this concept provided a very promising way to design efficient OHEs for waste heat recovery.

AUTHOR INFORMATION

Corresponding Authors:

Prof. Xiao Hu
Address: School of Materials Science & Engineering, Nanyang Technological University. N4.1-01-14, 50 Nanyang Avenue, Singapore 639798.
Phone: +65 6790 4610
Fax: +65 6790 9081
Email: Asxhu@ntu.edu.sg

Prof. Zhiping Lai
Address: Al-Jazri Building (Building 4), Room 4218, 4700 King Abdullah University of Science and Technology. Thuwal, 23955-6900, Kingdom of Saudi Arabia.
Phone: +966 12 8082408
Fax: +966 12 802 1328
Email: Zhiping.lai@kaust.edu.sa

AUTHOR CONTRIBUTIONS

Y. Zhong and X. Wang did most of the experimental measurements and data analyses. S. Telalovic contributed to the heat of capacity measurements. Z. Lai prepared the manuscript. Z. Lai, and X. Hu conceived the TRIL-OHE concept. X. Feng, K-W. Huang and Y. Gnanou contributed to the design of the thermally responsive ILs.

ACKNOWLEDGEMENTS

The work was supported by KAUST competitive research grant URF/1/1723.

ABBREVIATIONS

α phase, water-rich phase; β phase, ionic liquid –rich phase; CM, capacitance mixing; FO, forward osmosis; IL, Ionic liquids; TRIL, thermally responsive ionic liquid; LCST, lower critical solution temperature; UCST, upper critical solution temperature; OHE, osmotic heat engine; PD, power density; RED, reverse electro dialysis; SE, specific energy; SGE, salinity gradient energy; Tc, critical temperature; T_0, initial temperature; T_K, working temperature; TFC, thin film composite.

REFERENCES

1. BCS Incorporated, *Waste heat recovery: technology and opportunities in US industry*; 2008.
2. Alexander, S. R.; Srinivas, G., Energy harvesting, reuse and upgrade to reduce primary energy usage in the USA. *Energy* **2011,** *36*, 6172-6183.
3. Loeb, S. Method and apparatus for generating power utilizing pressure-retarded osmosis. US Patent 3906250, 1975.
4. Logan, B. E.; Elimelech, M., Membrane-based processes for sustainable power generation using water. *Nature* **2012,** *488*, 313-319.
5. Carati, A.; Marino, M.; Brogioli, D., Thermodynamic study of a distiller-electrochemical cell system for energy production from low temperature heat sources. *Energy* **2015,** *93, Part 1*, 984-993.
6. Dean, J. A.; Lange, N. A.; Dean, J. A., *Lange's Handbook of Chemistry*. McGraw-Hill: 1992.
7. McGinnis, R. L.; McCutcheon, J. R.; Elimelech, M., A Novel Ammonia-Carbon Dioxide Osmotic Heat Engine for Power Generation. *J. Membr. Sci.* **2007,** *305*, 13-19.
8. Weinstein, J. N.; Leitz, F. B., Electric power from differences in salinity: the dyalitic battery. *Science* **1976,** *191*, 557-559.
9. Quickenden, T. I.; Mua, Y., A review of power generation in aqueous thermogalvanic cells. *J. Electrochem. Soc.* **1995,** *142*, (11), 3985-3994.

10. Ponce de Leon, C.; Frias-Ferrer, A.; Gonzalez-Garcia, J.; Szanto, D. A.; Walsh, F. C., Redox flow cells for energy conversion. *J. Power Sources* **2006,** *160*, (1), 716-732.
11. Rica, R. A.; Ziano, R.; Salerno, D.; Mantegazza, F.; van Roij, R.; Brogioli, D., Capacitive mixing for harvesting the free energy of solutions at different concentrations. *Entropy* **2013,** *15*, (4), 1388-1407.
12. Peljo, P.; Lloyd, D.; Nguyet, D.; Majaneva, M.; Kontturi, K., Towards a thermally regenerative all-copper redox flow battery. *Phys. Chem. Chem. Phys.* **2014,** *16*, 2831-2835.
13. Zhang, F.; Liu, J.; Yang, W. L.; Logn, B. E., A thermally regenerative ammonia-based battery for efficient harvesting of low-grade thermal energy as electrical power. *Energy Environ. Sci.* **2015,** *8*, 343-349.
14. Kim, J. J.; Chung, J. S.; Kang, H.; Yu, Y. A.; Choi, W. J.; Kim, H. J.; Lee, J. C., Thermo-responsive copolymers with ionic group as novel draw solutes for forward osmosis processes. *Macromol. Res.* **2014,** *22*, (9), 963-970.
15. Zhu, X.; Rahimi, M.; Gorski, C. A.; Logn, B. E., A Thermally-Regenerative Ammonia-Based Flow Battery for Electrical Energy Recovery from Waste Heat. *ChemSusChem* **2016,** *9*, 873-879.
16. Marino, M.; Misuri, L.; Carati, A.; Brogioli, D., Proof-of-Concept of a Zinc-Silver Battery for the Extraction of Energy from a Concentration Difference. *Energies* **2014,** *7*, 3664-3683.
17. Flieger, J.; Czaijkowska-Zelazko, A., Ionic Liquids in separation techniques. In *Applications of ionic liquids in science and technology*, Handy, S., Ed. InTech: 2011.
18. Werner, S.; Haumann, M.; Wasserscheid, P., Ionic Liquids in Chemical Engineering. *Annu. Rev. Chem. Biomol. Eng.* **2010,** *1*, 203-230.
19. Cai, Y. F.; Shen, W. M.; Wei, J.; Chong, T. H.; Wang, R.; Krantz, W. B.; Fane, A. G.; Hu, X., Energy-efficient desalination by forward osmosis using responsive ionic liquid draw solutes. *Environ. Sci.: Water Res. Technol.* **2015,** *1*, 341-347.
20. Zhong, Y.; Feng, X.; Chen, W.; Wang, X.; Huang, K. W.; Gananou, Y.; Lai, Z. P., Using UCST ionic liquid as a draw solute in forward osmosis to treat high-salinity water. *Environ. Sci. Technol.* **2016,** *50*, 1039-1045.
21. Cai, Y. F.; Hu, X., A Critical review on draw solutes development for forward osmosis. *Desalination* **2016,** *391*, 16-29.
22. Straub, A. P.; Deshmukh, A.; Elimelech, M., Pressure-retarded osmosis for power generation from salinity gradients: is it viable? *Energy Environ. Sci.* **2016,** *9*, 31-48.
23. Yip, N. Y.; Elimelech, M., Comparison of energy efficiency and power density in pressure retarded osmosis and reverse electrodialysis. *Environ. Sci. Technol.* **2014,** *48*, 11002-11012.
24. Rebelo, L. P. N.; Najdanovic-Visak, V.; Visak, Z. P.; Nunes da Ponte, M.; Szydlowski, J.; Cerdeirina, C. A.; Troncoso, J.; Romani, L.; Esperanca, J. M. S. S.; Guedes, H. J. R.; de Sousa, H. C., A detailed thermodynamic analysis of [C_4mim][BF_4] + water as a case study to model ionic liquid aqueous solutions. *Green Chem.* **2004,** *6*, 369-381.
25. Bendova, M.; Wagner, Z., Thermodynamic descriptionof liquid-liquid equilibria in systems 1-thyl-3-methylimidazolium ethylsufate+C7-hydrocarbons by polymer-solution models. *Fluid Phase Equilibria* **2009,** *284*, 80-85.
26. Lei, Z. G.; Dai, C. N.; Liu, X.; Xiao, L.; Chen, B. H., Extension of the UNIFAC model for ionic liquids. *Ind. Eng. Chem. Res.* **2012,** *51*, 12135-12144.
27. Pitzer, K. S.; Peiper, J. C.; Busey, R. H., Thermodynamic properties of aqueous sodium chloride solutions. *J. Phys. Chem. Ref. Data* **1984,** *13*, (1), 3-102.
28. Lin, S. H.; Straub, A. P.; Elimelech, M., Thermodynamic limits of extractable energy by pressure retarded osmosis. *Energy Environ. Sci.* **2014,** *7*, 2706-2714.
29. Achilli, A.; Prante, J. L.; Hancock, N. T.; Maxwell, E. B.; Childress, A. E., Experimental Results from RO-PRO: A Next Generation System for Low-Energy Desalination. *Environ. Sci. Technol.* **2014,** *48*, (11), 6437-6443.
30. Ramon, G. Z.; Feinberg, B. J.; Hoek, E. M. V., Membrane-based production of salinity-gradient power. *Energy Environ. Sci.* **2011,** *4*, (11), 4423-4434.

31. Yip, N. Y.; Tiraferri, A.; Phillip, W. A.; Schiffman, J. D.; Hoover, L. A.; Kim, Y. C.; Elimelech, M., Thin-Film Composite Pressure Retarded Osmosis Membranes for Sustainable Power Generation from Salinity Gradients. *Environ Sci Technol* **2011,** *45*, (10), 4360-4369.
32. Straub, A. P.; Yip, N. Y.; Elimelech, M., Raising the Bar: Increased Hydraulic Pressure Allows Unprecedented High Power Densities in Pressure-Retarded Osmosis. *Environ. Sci. Technol. Lett.* **2014,** *1*, (1), 55-59.
33. Han, G.; Zhang, S.; Li, X.; Chung, T.-S., High performance thin film composite pressure retarded osmosis (PRO) membranes for renewable salinity-gradient energy generation. *J. Membr. Sci.* **2013,** *440*, 108-121.
34. Gerstandt, K.; Peinemann, K. V.; Skilhagen, s. E.; Thorsen, T.; Holt, T., Membrane Processes in energy Supply for an Osmotic Power Plant. *Desalination* **2008,** *224*, 64-70.

419 **Table of Contents and Graphic Synopsis**

420

421